ACS Photonics

Article

Cite This: ACS Photonics 2018, 5, 3082−3088

Exploring the Limits of Super-Planckian Far-Field Radiative Heat Transfer Using 2D Materials

Víctor Fernández-Hurtado,*[,†,‡] Antonio I. Fernández-Domínguez,[†] Johannes Feist,[†] Francisco J. García-Vidal,[†,§] and Juan Carlos Cuevas[†,‡]

[†]Departamento de Física Teórica de la Materia Condensada and Condensed Matter Physics Center (IFIMAC), Universidad Autónoma de Madrid, E-28049 Madrid, Spain

[‡]Department of Physics, University of Konstanz, D-78457 Konstanz, Germany

[§]Donostia International Physics Center (DIPC), Donostia/San Sebastián 20018, Spain

Supporting Information

ABSTRACT: Very recently it has been predicted that the far-field radiative heat transfer between two macroscopic systems can largely overcome the limit set by Planck's law if one of their dimensions becomes much smaller than the thermal wavelength ($\lambda_{Th} \approx 10$ μm at room temperature). To explore the ultimate limit of the far-field violation of Planck's law, here we present a theoretical study of the radiative heat transfer between two-dimensional (2D) materials. We show that the far-field thermal radiation exchanged by two coplanar systems with a one-atom-thick geometrical cross section can be more than 7 orders of magnitude larger than the theoretical limit set by Planck's law for blackbodies and can be comparable to the heat transfer of two parallel sheets at the same distance. In particular, we illustrate this phenomenon with different materials such as graphene, where the radiation can also be tuned by a external gate, and single-layer black phosphorus. In both cases the far-field radiative heat transfer is dominated by TE-polarized guiding modes, and surface plasmons play no role. Our predictions provide a new insight into the thermal radiation exchange mechanisms between 2D materials.

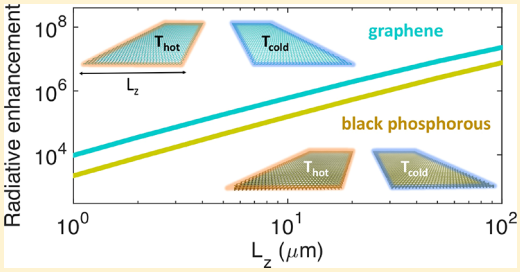

KEYWORDS: *radiative heat transfer, 2D materials, super-Planckian, far-field, graphene, black phosphorus*

Radiation is, together with convection and conduction, one of the three basic mechanisms of heat exchange between bodies.[1] The maximum thermal energy that can be transferred between two objects via radiation is, in principle, set by Planck's law for blackbodies,[2] which assumes that both of them are perfect absorbers at all frequencies and that all dimensions involved in the problem are larger than λ_{Th}. However, it is known that when the separation between two bodies is smaller than λ_{Th}, the radiative heat transfer can be enhanced by orders of magnitude due to the contribution of evanescent waves.[3−7] This phenomenon, known as near-field radiative heat transfer (NFRHT),[3,4] has been confirmed in recent years by several experiments exploring different geometries, materials, and distances between the two objects, ranging from micrometers down to a few nanometers.[8−22] On the other hand, Planck's law is also expected to fail when objects have dimensions smaller than λ_{Th}, even in the far field. In this case, nothing prevents, in principle, overcoming the Planckian limit. In fact, it has been predicted that the far-field thermal emission of a single object can be super-Planckian,[23−26] but in practice this is very difficult to achieve, and this phenomenon has never been observed. In the context of radiative heat transfer, which is the problem that we are interested in, only very recently have we predicted that the Planckian limit can also be largely surpassed in the far-field regime,[27] i.e., when the separation of the objects is larger than λ_{Th}. In particular, we have shown theoretically that the far-field radiative heat transfer (FFRHT) between micrometer-size devices can overcome the blackbody limit by several orders of magnitude if their thickness is much smaller than λ_{Th}. Moreover, we have shown that the enhancement over Planck's law increases monotonically as the device thickness is reduced,[27] which leads us to the fundamental question on the limits of super-Planckian FFRHT. The goal of this work is to explore this issue with the help of 2D materials, i.e., with materials with a one-atom-thick geometrical cross section, which constitutes the ultimate limit of thin systems.

2D materials have been extensively studied in recent years in the context of radiative heat transfer. In particular, several works have taken advantage of the near-field density of photonic states in these systems to modify the characteristics of emitters in a wide variety of scenarios. Most of the theoretical work in the case of graphene has focused on the possibility to tune and enhance the NFRHT mediated by the surface plasmon−polaritons sustained by this material.[28,29] For instance, it has been predicted that the NFRHT between polar

Received: March 13, 2018
Published: June 19, 2018

DOI: 10.1021/acsphotonics.8b00328
ACS Photonics 2018, 5, 3082−3088

dielectrics can be boosted by placing a graphene layer on top.[30−32] This prediction has been confirmed experimentally.[33] Other studies have proposed periodic graphene ribbon arrays to induce hyperbolic modes and thus further enhance the NFRHT between 2D systems.[34] The NFRHT between graphene nanodisks has also been studied,[35] and the analysis of the time scales of radiative heat transfer in this setup suggests that this process is ultrafast.[36] Let us also mention that the near-field thermal conductance between Dirac 2D materials scales as the inverse of the distance between two flakes.[37] However, and despite all these recent advances, FFRHT between 2D materials remains unexplored. As explained above, 2D materials constitute ideal systems in which one can explore the ultimate limit of the violation of Planck's law in the far-field regime. Moreover, from an applied viewpoint, understanding the absorption and emission of radiation in 2D materials is key to properly characterize their thermal properties and harness their unique mechanical and electronic features.[38] For these reasons, we present in this work a theoretical study of the FFRHT between systems with a one-atom-thick geometrical cross section. In particular, we demonstrate that the FFRHT between sheets of 2D materials like graphene or single-layer black phosphorus can overcome the Planckian limit by more than 7 orders of magnitude. Moreover, we show that, contrary to the known NFRHT mechanism, surface plasmon−polaritons play no role in this case, and this remarkable heat transfer is instead dominated by TE-polarized guiding modes.

RESULTS AND DISCUSSION

Let us start by analyzing the FFRHT between two coplanar graphene sheets. This system is schematically represented in Figure 1a. In this case, two identical graphene sheets at temperatures T_1 and T_2 ($T_1 < T_2$) are separated by a gap d. The length of the flakes is denoted by L_z, and, for simplicity, we shall assume that they are infinitely wide in the x-direction ($L_x \to \infty$). Notice that, as shown in Figure 1a, both flakes are coplanar, and thus, for the radiative problem they constitute systems with a one-atom-thick geometrical cross section. In order to compute the power exchanged in the form of thermal radiation between these 2D systems, we make use of the theory of fluctuational electrodynamics.[4,5] In this theory, the material properties enter via the dielectric function, which in the graphene case can be determined from the electrical conductivity.[39] The 2D conductivity of graphene, $\sigma_{2D}^{graphene}$, calculated within the random phase approximation can be expressed in terms of the chemical potential (μ), temperature (T), and scattering energy ($\mathcal{E}_s$)[40]

$$\sigma_{2D}^{graphene} = \sigma_{intra} + \sigma_{inter} \tag{1}$$

where the intraband and the interband contributions are given by

$$\sigma_{intra} = \frac{2ie^2 t}{\hbar\pi(\Omega + i\gamma)} \ln\left[2\cosh\left(\frac{1}{2t}\right)\right],$$

$$\sigma_{inter} = \frac{e^2}{4\hbar}\left[\frac{1}{2} + \frac{1}{\pi}\arctan\left(\frac{\Omega - 2}{2t}\right) - \frac{i}{2\pi}\ln\frac{(\Omega + 2)^2}{(\Omega - 2)^2 + (2t)^2}\right] \tag{2}$$

with $\Omega = \hbar\omega/\mu$, $\gamma = \mathcal{E}_s/\mu$, and $t = k_B T/\mu$. In Figure 1b we show the normalized 2D conductivity of graphene, in units of $\sigma_0 = e^2/2\pi\hbar$, for $T = 300$ K, $\mathcal{E}_s = 10^{-4}$ eV, and different values of the chemical potential. As one can see, graphene resembles a Drude metal in the infrared regime whose metallic character increases with the chemical potential. Let us remark that the value chosen in this case for $\mathcal{E}_s$ corresponds to a graphene sheet with a very large relaxation time, $\tau = \hbar/\mathcal{E}_s$, which is normally the desired scenario in the field of graphene plasmonics.[41] We will show below that the opposite limit is indeed more favorable for the absorption and emission of radiation between 2D materials.

In order to calculate the FFRHT, we make use of a result derived in a recent work[27] with the help of a thermal discrete dipole approximation.[42] This result establishes a connection between the FFRHT between two objects and their absorption efficiencies, i.e., their absorption cross sections divided by their geometrical cross sections. Assuming that a sheet of a 2D material can be modeled as a parallelepiped (see below), this result indicates that the radiative power exchanged between two identical flakes at temperatures T_1 and T_2 and separated by a gap d much larger than both λ_{Th} and their characteristic dimensions is given by[27]

$$P = \frac{\pi}{2} A F_{12} \int_0^\infty [Q_{TE}^2(\omega) + Q_{TM}^2(\omega)][I_{BB}(\omega, T_1) - I_{BB}(\omega, T_2)]\, d\omega \tag{3}$$

where A is the geometrical cross section of the bodies and $F_{12} = \delta/2d$ is the geometrical view factor,[1] where δ is the geometric thickness of the 2D material. On the other hand, $Q_{TM,TE}(\omega)$ is the frequency-dependent absorption efficiency for a plane wave with normal incidence and transverse magnetic (TM) or

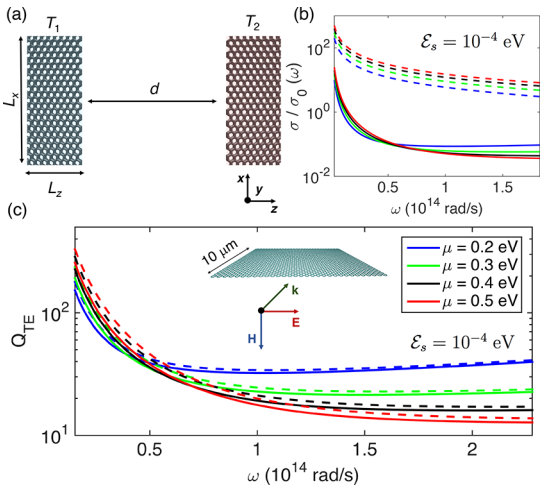

Figure 1. (a) Schematics of the FFRHT between two identical graphene flakes. The flakes have dimensions $L_x \times L_z$, are separated by a gap d, and are held at temperatures T_1 and T_2, respectively. (b) Real (solid lines) and imaginary (dashed lines) part of the normalized conductivity for $T = 300$ K, $\mathcal{E}_s = 10^{-4}$ eV, and for different chemical potentials (μ), as indicated in the legend of panel (c). (c) Frequency-dependent absorption efficiency for a plane wave with transverse electric polarization ($Q_{TE}(\omega)$) and normal incidence into a graphene sheet with length $L_z = 10$ μm, infinite width (see inset), and for different values of μ (see legend). The solid lines correspond to the exact numerical results, while the dashed lines correspond to the results obtained with eq 5.

DOI: 10.1021/acsphotonics.8b00328
ACS Photonics 2018, 5, 3082−3088

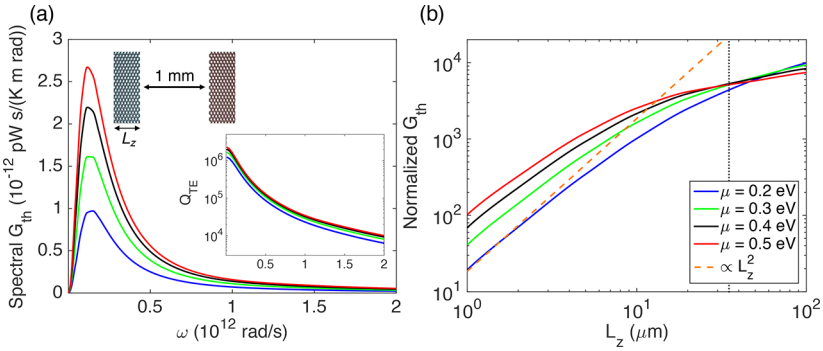

Figure 2. (a) Spectral thermal conductance as a function of the radiation frequency for a system composed of two graphene flakes of length L_z = 10 μm, $\mathcal{E}_s = 10^{-4}$ eV, and a gap d = 1 mm (see upper inset). The different lines correspond to distinct chemical potentials (see legend in (b)), and the temperature is 300 K. The lower inset shows the corresponding absorption efficiency $Q_{TE}(\omega)$ in the same frequency range as the spectral conductance. (b) Total thermal conductance G_{th}, normalized by the blackbody results, for the same system as in panel (a) and plotted as a function of L_z for different chemical potentials. The dashed orange line is proportional to L_z^2. The vertical dotted line indicates approximately the length at which the conductance for μ = 0.5 eV starts to saturate (see text). Let us stress that these normalized results do not depend on the gap as long as d is much larger than the thermal wavelength.

transverse electric (TE) polarization, and $I_{BB}(\omega, T)$ is the Planck distribution function, which is given by

$$I_{BB}(\omega, T) = \frac{\omega^2}{4\pi^3 c^2} \frac{\hbar\omega}{\exp(\hbar\omega/k_B T) - 1} \tag{4}$$

where c is the speed of light. The blackbody limit can be obtained by assuming that the absorption efficiencies $Q_{TM,TE}(\omega) = 1$ for all frequencies. In this case, eq 3 reduces to the Stefan–Boltzmann law:[1] $P_{BB} = \sigma A F_{12}(T_1^4 - T_2^4)$, where $\sigma = 5.67 \times 10^{-8}$ W/(m^2 K^4). It is worth mentioning that we have verified the validity of eq 3 to calculate the FFRHT between 2D materials by comparing its results with numerically exact simulations within the framework of fluctuational electrodynamics (Supporting Information, Figure S1).

According to eq 3, $Q_{TM,TE}(\omega)$ are required to calculate the FFRHT between two graphene sheets. Since our system is one atom thick in the y-direction (Figure 1a), a wave impinging with the electric field pointing in the y-direction does not generate any current in that direction. Hence, the absorption cross section of TM plane waves vanishes ($Q_{TM}(\omega) = 0$), and only $Q_{TE}(\omega)$ contributes to the FFRHT. Note that free-space propagating waves cannot couple efficiently to surface plasmons in graphene, which lie far outside the light line, due to the large mismatch in in-plane momentum. We have calculated this efficiency using COMSOL MULTIPHYSICS, where we have modeled our system as a 3D parallelepiped with an effective dielectric constant[39] (see Supporting Information). In accordance with experimental evidence, we have taken $\delta_{graphene}$ = 0.37 nm for the thickness of a graphene monolayer.[43] Figure 1c shows $Q_{TE}(\omega)$ as a function of the radiation frequency ω (solid lines) for different chemical potentials and for a scattering energy $\mathcal{E}_s = 10^{-4}$ eV. Notice that the absorption cross section is much larger than the geometrical one in the infrared frequency range, which shows that graphene is a very efficient broadband infrared absorber, even when the incident vector of the plane wave is parallel to the graphene sheet (see inset in Figure 1c). Notice also that $Q_{TE}(\omega)$ increases for decreasing frequency, which is due to the increase of losses in the system (see Figure 1b).

In order to get further insight into the remarkable radiation absorption of a graphene flake, we have derived an analytical expression for $Q_{TE}(\omega)$ in eq 3 as follows. The radiation absorption can be understood as a two-step process. First, a TE plane wave impinges in the graphene flake (see inset in Figure 1c) and couples to the guiding modes of our system. Second, these modes propagate along the z-direction, while being progressively absorbed by the graphene flake. Taking both processes into account (Supporting Information, Figure S2), the frequency-dependent absorption efficiency can be expressed as

$$Q_{TE}^{an}(\omega) = \frac{1 - e^{-2\mathrm{Im}\{k_z\}L_z}}{\delta \mathrm{Im}\{k_{y,v}\}} \tag{5}$$

Here, k_z corresponds to the z-component of the graphene mode wave vector and $k_{y,v}$ represents the y-component of the same wave vector in a vacuum. In eq 5, the factor $1/\mathrm{Im}\{k_{y,v}\}$ is related to the coupling between the plane wave and the EM mode of the system, while the numerator $(1 - e^{-2\mathrm{Im}\{k_z\}L_z})$ accounts for the absorption of the guiding wave along the graphene sheet. We have computed the dispersion relation of the leaky guided modes of our system by using standard dielectric waveguide theory[44] (see Supporting Information). In Figure 1c we show the analytical results for the absorption efficiency $Q_{TE}^{an}(\omega)$ (dashed lines), and, as one can see, there is an excellent agreement with the exact numerical simulations. This agreement allows us to conclude that the extraordinary absorption efficiency of a graphene flake in this configuration is due to the fact that it behaves as a lossy waveguide that absorbs the radiation via the excitation of guided TE modes. In particular, because of the low impedance mismatch, the incident radiation is efficiently coupled into guided modes and is eventually absorbed.

Once $Q_{TE}(\omega)$ is known, we can use eq 3 to calculate the FFRHT between two graphene flakes in the coplanar configuration (see Figure 1a). We shall characterize the FFRHT in terms of the room-temperature linear heat conductance per unit of length, $G_{th} = P/(L_x \Delta T)$, in the limit $\Delta T = (T_2 - T_1) \to 0$. Figure 2a shows the spectral G_{th}, i.e., the conductance per unit of frequency, for two graphene sheets of length L_z = 10 μm, $\mathcal{E}_s = 10^{-4}$ eV, and a gap d = 1 mm. It can be observed that the system exhibits a broadband FFRHT spectrum, similar to the FFRHT between metals.[3] The conductance peak appears at $\omega = 9 \times 10^{10}$ rad/s for all chemical potentials. This maximum originates from the

DOI: 10.1021/acsphotonics.8b00328
ACS Photonics 2018, 5, 3082–3088

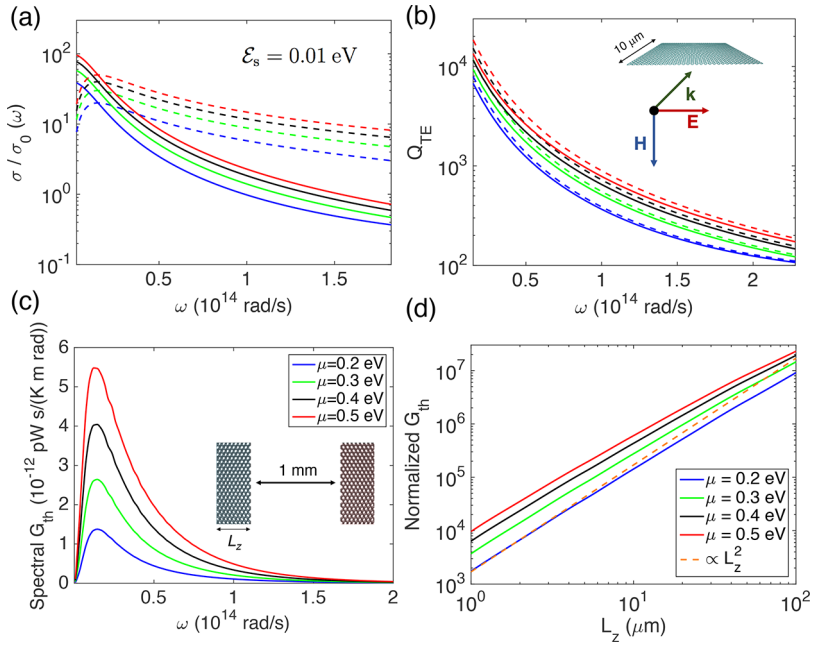

Figure 3. (a) Real (solid lines) and imaginary (dashed lines) part of the normalized conductivity of graphene for $T = 300$ K and $\mathcal{E}_s = 0.01$ eV, for different chemical potentials (μ). (b) Frequency-dependent absorption efficiency for a plane wave with transverse electric polarization ($Q_{TE}(\omega)$) and normal incidence into a graphene sheet with length $L_z = 10$ μm and infinite width (see inset), for different values of μ. The solid lines correspond to the exact numerical results, while the dashed lines were obtained with eq 5. (c) Spectral G_{th} as a function of ω for a system composed of two graphene flakes of length $L_z = 10$ μm, $\mathcal{E}_s = 0.01$ eV, and a gap $d = 1$ mm (see inset). (d) G_{th}, normalized by the blackbody results, for the same system and plotted as a function of L_z for different chemical potentials. The dashed orange line is proportional to L_z^2.

convolution of the Planck's distribution function (I_{BB}) and $Q_{TE}(\omega)$; see eq 3. Notice, however, that the magnitude of G_{th} does increase with μ and can be tuned by a factor of 2.5 between $\mu = 0.2$ eV and $\mu = 0.5$ eV.

Let us turn now to the analysis of the total thermal conductance and its comparison with the predictions of Planck's law for blackbodies. Figure 2b shows G_{th} normalized by the corresponding blackbody result ($G_{BB} = 4\sigma\delta F_{12}T^3$) as a function of the flake's length L_z. Let us stress that in all the calculations of the thermal conductance based on eq 3, we have computed the absorption efficiencies numerically with COMSOL MULTIPHYSICS. As it can be observed, the power exchanged by the two graphene flakes overcomes Planck's results by up to 4 orders of magnitude for a length of 100 μm. The reason for this huge enhancement can be understood with the help of Figure 1c, where it is shown that the absorption efficiency of a graphene sheet reaches values much larger than 1 for a broad range of infrared frequencies, accessible at room temperature. Besides, the normalized G_{th} increases with L_z simply because the absorption and emission of radiation in the graphene flakes increase with this length. It can be also seen in Figure 2b that for small lengths the normalized G_{th} is proportional to L_z^2, which can be understood as follows. The efficiency $Q_{TE}(\omega)$ is proportional to $(1 - e^{-2\mathrm{Im}\{k_z\}L_z})$, according to eq 5. In the limit in which $\mathrm{Im}\{k_z\}L_z \ll 1$, $Q_{TE}(\omega)$ is simply proportional to L_z. Thus, from eq 3, it is obvious that $G_{th} \propto L_z^2$ for short graphene flakes, as verified in Figure 2b. In the opposite limit, i.e., when the length of the flake becomes very large, the normalized thermal conductance tends to saturate; see Figure 2b. In this case, the analysis of even longer flakes becomes very challenging from the numerical point of view. The transition between these two regimes occurs approximately at $L_z \approx 1/(2\mathrm{Im}\{k_z\})$, which is indicated by a vertical dotted line in Figure 2b for $\mu = 0.5$ eV. This length was calculated for the frequency at which the spectral conductance reaches its maximum ($\omega = 1.2 \times 10^{11}$ rad/s).

We have shown that the FFRHT between graphene sheets can overcome the Planckian limit by more than 4 orders of magnitude. However, our analysis also suggests that the thermal conductance could be further enhanced by increasing the intrinsic losses in the graphene sheets. To test this idea, we have calculated the FFRHT for these graphene sheets assuming a larger value for the scattering energy $\mathcal{E}_s$. Figure 3a shows the normalized 2D conductivity of graphene for $\mathcal{E}_s = 0.01$ eV, i.e., 2 orders of magnitude larger than in the examples above. The corresponding results for the absorption efficiency $Q_{TE}(\omega)$ are displayed in Figure 3b. The absorption cross section is again orders of magnitude larger than the geometrical one, and, more importantly, it is also higher than in the previous case. Figure 3c shows the spectral G_{th} for $L_z = 10$ μm, $\mathcal{E}_s = 0.01$ eV, and a gap $d = 1$ mm. In this case the maximum of the spectral G_{th} is strongly blue-shifted ($\omega = 1.3 \times 10^{13}$ rad/s), and the relevant frequencies for the FFRHT are also higher. The reason for this blue-shift is that $Q_{TE}(\omega)$ adopts larger values at frequencies that have a better overlap with Planck distribution function at room temperature. As a consequence, the total thermal conductance G_{th} is much higher in this case, as we illustrate in Figure 3d. Notice that in this case the Planckian limit can be overcome by more than 7 orders of magnitude. Thus, we see here that the graphene with a high density of impurities (i.e., with low mobility), which is normally dismissed for optoelectronic and plasmonic applications, is more efficient regarding thermal emission and absorption.

For the sake of comparison, we have also analyzed the FFRHT between two graphene sheets of the same dimensions as those of Figure 3c ($\mu = 0.3$ eV) now parallel to each other

DOI: 10.1021/acsphotonics.8b00328
ACS Photonics 2018, 5, 3082−3088

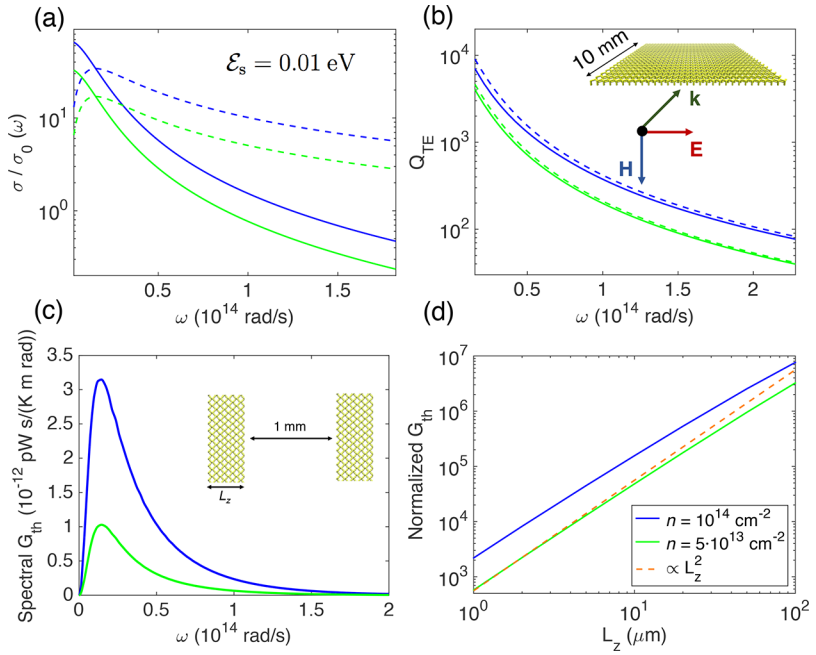

Figure 4. (a) Real (solid lines) and imaginary (dashed lines) part of the normalized conductivity of single-layer black phosphorus for T = 300 K and $\mathcal{E}_s$ = 0.01 eV, for two different dopings (n). (b) Frequency-dependent absorption efficiency for a plane wave with transverse electric polarization ($Q_{TE}(\omega)$) and normal incidence into an SLBP sheet with length L_z = 10 μm and infinite width (see inset). The solid lines correspond to the exact numerical results, while the dashed lines were obtained with eq 5. (c) Spectral G_{th} as a function of ω for a system composed of two SLBP flakes of length L_z = 10 μm separated by a gap d = 1 mm (see inset). (d) Thermal conductance G_{th}, normalized by the blackbody results, for the same system as in panel (c) and plotted as a function of L_z, for two different dopings. The dashed orange line is proportional to L_z^2.

and separated by a distance d along the normal direction. In that case, the geometrical cross section is 27 000 times larger than in the coplanar configuration and Planck's law would thus predict 27 000^2 higher heat transfer efficiency than in the coplanar case. However, the FFRHT between the graphene sheets in this case is only 4 times larger, and it does not exhibit an enhancement over Planck's law. Indeed, the ratio with the blackbody results is 1.5×10^{-3}. This confirms that the FFRHT between coplanar sheets is truly remarkable and that its absolute value is comparable with other setups that have a much higher geometrical cross section. Moreover, we have performed additional simulations to verify if such FFRHT could be measured in a realistic experimental setup. We have calculated the FFRHT between two graphene sheets with L_x = 20 μm, L_z = 60 μm, μ = 0.5 eV, and $\mathcal{E}_s$ = 0.01 eV and separated by a gap of 20 μm, where the thermal radiation is already dominated by the far-field contribution.[7] The dimensions chosen for both the graphene sheets and the gap are within reach of state-of-the-art calorimetric techniques.[47,48] In order to compute the FFRHT, we have made use of the code SCUFF-EM, which implements a fluctuating-surface-current approach to the radiative heat transfer problem and provides numerically exact results within the framework of fluctuational electrodynamics.[45,46] The room-temperature linear heat conductance between the flakes is in this case 1.62 pW/K, which is within the sensitivity of existent calorimetric techniques.[47,48]

At this point one may wonder whether the dramatic violation of Planck's law discussed above for the case of graphene may also occur in other 2D materials. To show that this is actually the case, we now turn to analyze the case of single-layer black phosphorus (SLBP). We have computed the FFRHT between two coplanar SLBP sheets (see Figure 1a). The distinctive steps of the atomic structure of SLBP are in our case placed along the z-direction. We have modeled the dielectric properties of a black phosphorus monolayer in an analogous way to graphene, and its 2D conductivity has been taken from previous studies.[49] Both the real (solid line) and the imaginary (dashed line) part of the conductivity of SLBP along the x-direction are plotted in Figure 4a for T = 300 K, $\mathcal{E}_s$ = 0.01 eV, and two different electron dopings $n = 5 \times 10^{13}$ cm^{-2} and $n = 10^{14}$ cm^{-2}. The parameters chosen represent realistic SLBP samples.[50] Figure 4b shows $Q_{TE}(\omega)$ calculated numerically (solid lines) with COMSOL MULTIPHYSICS (see Supporting Information) for a SLBP sheet with L_z = 10 μm (see inset of Figure 4b) and both doping values. The SLBP absorption efficiency exhibits very similar characteristics to those of low-quality graphene, as both of them have similar dielectric functions for infrared frequencies. Moreover, $Q_{TE}^{an}(\omega)$ (dashed lines) shows again an excellent agreement with the exact numerical simulations. As for graphene, we have used the results for $Q_{TE}(\omega)$ in combination with eq 3 to describe the FFRHT. The spectral conductance of black phosphorus monolayers separated by 1 mm is plotted in Figure 4c, while the normalized total thermal conductance as a function of the length L_z is shown in Figure 4d. Notice that in this case the FFRHT can be larger than the corresponding result calculated from Planck's law by almost 7 orders of magnitude, showing that this enhancement is not exclusive of graphene, but can also occur in other 2D materials such as SLBP.

In summary, we have presented a theoretical analysis of the FFRHT between 2D materials, graphene, and single-layer black phosphorus, in a coplanar configuration. We have shown that the relevant absorption cross section of flakes of these materials can be orders of magnitude larger than their atomic-sized geometrical cross section. We have also shown that this

DOI: 10.1021/acsphotonics.8b00328
ACS Photonics 2018, 5, 3082−3088

extraordinary absorption efficiency makes the FFRHT between flakes of these materials more than 7 orders of magnitude larger than the limit set by Planck's law, which constitutes the ultimate violation of this law in the far-field regime. Finally, we have shown that the novel mechanism responsible for this FFRHT involves the propagation properties of TE-polarized guiding modes in these materials, modes that are usually irrelevant in the context of plasmonic or optoelectronic applications.

■ ASSOCIATED CONTENT

Supporting Information

The Supporting Information is available free of charge on the ACS Publications website at DOI: 10.1021/acsphotonics.8b00328.

Proof of the validity of eq 3 to calculate the FFRHT between 2D materials, details on the modeling of 2D materials as 3D parallelepipeds, and the derivation of eq 5 (PDF)

■ AUTHOR INFORMATION

Corresponding Author

*E-mail: victor.fernandezh@uam.es.

ORCID

Víctor Fernández-Hurtado: 0000-0002-0102-9011
Antonio I. Fernández-Domínguez: 0000-0002-8082-395X
Johannes Feist: 0000-0002-7972-0646
Francisco J. García-Vidal: 0000-0003-4354-0982

Notes

The authors declare no competing financial interest.

■ ACKNOWLEDGMENTS

This work has been financially supported by the Spanish MINECO (FIS2015-64951-R, MAT2014-53432-C5-5-R, and FIS2017-84057-P), the Comunidad de Madrid (S2013/MIT-2740), the European Union Seventh Framework Programme (FP7-PEOPLE-2013-CIG-630996), and the European Research Council (ERC-2011-AdG-290981 and ERC-2016-STG-714870). V.F.-H. acknowledges support from "la Caixa" Foundation. V.F.-H. and J.C.C. (Mercator Fellow) thank the DFG and SFB767 for sponsoring their stay at the University of Konstanz.

■ REFERENCES

(1) Bergman, T. L.; Lavine, A. S.; Incropera, F. P.; Dewitt, D. P. *Fundamentals of Heat and Mass Transfer*, 8th ed.; Wiley: New York, 2017.

(2) Planck, M. *The Theory of Thermal Radiation*; P. Blakiston Son & Co.: Philadelphia, 1914.

(3) Polder, D.; Van Hove, M. Theory of radiative heat transfer between closely spaced bodies. *Phys. Rev. B: Condens. Matter Mater. Phys.* **1971**, *4*, 3303−3314.

(4) Rytov, S. M.; Kravtsov, Y. A.; Tatarskii, V. I. *Principles of Statistical Radiophysics*, Vol. *3*; Springer-Verlag: Heidelberg, 1989.

(5) Joulain, K.; Mulet, J.-P.; Marquier, F.; Carminati, R.; Greffet, J.-J. Surface electromagnetic waves thermally excited: radiative heat transfer,coherence properties and casimir forces revisited in the near field. *Surf. Sci. Rep.* **2005**, *57*, 59−112.

(6) Basu, S.; Zhang, Z. M.; Fu, C. J. Review of near-field thermal radiation and its application to energy conversion. *Int. J. Energy Res.* **2009**, *33*, 1203−1232.

(7) Song, B.; Fiorino, A.; Meyhofer, E.; Reddy, P. Near-field radiative thermal transport: from theory to experiment. *AIP Adv.* **2015**, *5*, 053503.

(8) Kittel, A.; Müller-Hirsch, W.; Parisi, J.; Biehs, S.-A.; Reddig, D.; Holthaus, M. Near-field heat transfer in a scanning thermal Microscope. *Phys. Rev. Lett.* **2005**, *95*, 224301.

(9) Rousseau, E.; Siria, A.; Jourdan, G.; Volz, S.; Comin, F.; Chevrier, J.; Greffet, J.-J. Radiative heat transfer at the nanoscale. *Nat. Photonics* **2009**, *3*, 514−517.

(10) Shen, S.; Narayanaswamy, A.; Chen, G. Surface phonon polaritons mediated energy transfer between nanoscale gaps. *Nano Lett.* **2009**, *9*, 2909−2913.

(11) Ottens, R. S.; Quetschke, V.; Wise, S.; Alemi, A. A.; Lundock, R.; Mueller, G.; Reitze, D. H.; Tanner, D. B.; Whiting, B. F. Near-field radiative heat transfer between macroscopic planar surfaces. *Phys. Rev. Lett.* **2011**, *107*, 014301.

(12) Kralik, T.; Hanzelka, P.; Zobac, M.; Musilova, V.; Fort, T.; Horak, M. Strong near-field enhancement of radiative heat transfer between metallic surfaces. *Phys. Rev. Lett.* **2012**, *109*, 224302.

(13) van Zwol, P. J.; Ranno, L.; Chevrier, J. Tuning near field radiative heat flux through surface excitations with a metal insulator transition. *Phys. Rev. Lett.* **2012**, *108*, 234301.

(14) Worbes, L.; Hellmann, D.; Kittel, A. Enhanced near-field heat flow of a monolayer dielectric island. *Phys. Rev. Lett.* **2013**, *110*, 134302.

(15) St-Gelais, R.; Guha, B.; Zhu, L. X.; Fan, S.; Lipson, M. Demonstration of strong near-field radiative heat transfer betwee-nintegrated nanostructures. *Nano Lett.* **2014**, *14*, 6971−6975.

(16) Song, B.; Ganjeh, Y.; Sadat, S.; Thompson, D.; Fiorino, A.; Fernández-Hurtado, V.; Feist, J.; Garcia-Vidal, F. J.; Cuevas, J. C.; Reddy, P.; Meyhofer, E. Enhancement of near-field radiative heat transfer using polar dielectric thin films. *Nat. Nanotechnol.* **2015**, *10*, 253−258.

(17) Kim, K.; Song, B.; Fernández-Hurtado, V.; Lee, W.; Jeong, W.; Cui, L.; Thompson, D.; Feist, J.; Reid, M. T. H.; Garcia-Vidal, F. J.; Cuevas, J. C.; Meyhofer, E.; Reddy, P. Radiative heat transfer in the extreme near field. *Nature* **2015**, *528*, 387−391.

(18) St-Gelais, R.; Zhu, L.; Fan, S.; Lipson, M. Near-field radiative heat transfer between parallel structures in the deep subwavelength regime. *Nat. Nanotechnol.* **2016**, *11*, 515−519.

(19) Song, B.; Thompson, D.; Fiorino, A.; Ganjeh, Y.; Reddy, P.; Meyhofer, E. Radiative heat conductances between dielectric and metallic parallel plates with nanoscale gaps. *Nat. Nanotechnol.* **2016**, *11*, 509−514.

(20) Bernardi, M. P.; Milovich, D.; Francoeur, M. Radiative heat transfer exceeding the blackbody limit between macroscale planar surfaces separated by a nanosize vacuum gap. *Nat. Commun.* **2016**, *7*, 12900.

(21) Cui, L.; Jeong, W.; Fernández-Hurtado, V.; Feist, J.; García-Vidal, F. J.; Cuevas, J. C.; Meyhofer, E.; Reddy, P. Study of radiative heat transfer in Ångström- and nanometre-sized gaps. *Nat. Commun.* **2017**, *8*, 14479.

(22) Kloppstech, K.; Könne, N.; Biehs, S.-A.; Rodriguez, A. W.; Worbes, L.; Hellmann, D.; Kittel, A. Giant heat transfer in the crossover regime between conduction and radiation. *Nat. Commun.* **2017**, *8*, 14475.

(23) Kattawar, G. W.; Eisner, M. Radiation from a homogeneous isothermal sphere. *Appl. Opt.* **1970**, *9*, 2685−2690.

(24) Golik, V. A.; Krüger, M.; Kardar, M. Heat radiation from long cylindrical objets. *Phys. Rev. E: Stat. Nonlin. Soft Matter Phys.* **2012**, *85*, 046603.

(25) Biehs, S.-A.; Ben-Abdallah, P. Revisiting super-Planckian thermal emission in the far-field regime. *Phys. Rev. B: Condens. Matter Mater. Phys.* **2016**, *93*, 165405.

(26) Maslovski, S. I.; Simovski, C. R.; Tretyakov, S. A. Overcoming black body radiation limit in free space: metamaterial superemitter. *New J. Phys.* **2016**, *18*, 013034.

(27) Fernández-Hurtado, V.; Fernández-Domínguez, A. I.; Feist, J.; García-Vidal, F. J.; Cuevas, J. C. Super-Planckian far-field radiative

DOI: 10.1021/acsphotonics.8b00328
ACS Photonics 2018, 5, 3082−3088

heat transfer. *Phys. Rev. B: Condens. Matter Mater. Phys.* **2018**, *97*, 045408.
(28) Volokitin, A. I.; Persson, B. N. J. Near-field radiative heat transfer between closely spaced graphene and amorphous SiO_2. *Phys. Rev. B: Condens. Matter Mater. Phys.* **2011**, *83*, 241407.
(29) Ilic, O.; Marinko, J.; Joannopoulos, J. D.; Celanovic, I.; Buljan, H.; Soljačić, M. Near-field thermal radiation transfer controlled by plasmons in graphene. *Phys. Rev. B: Condens. Matter Mater. Phys.* **2012**, *85*, 155422.
(30) Stetovoy, V. B.; van Zwol, P. J.; Chevrier, J. Plasmon enhanced near-field radiative heat transfer for graphene covered dielectrics. *Phys. Rev. B: Condens. Matter Mater. Phys.* **2012**, *85*, 155418.
(31) Liu, X. L.; Zhang, Z. M. Graphene-assisted near-field radiative heat transfer between corrugated polar materials. *Appl. Phys. Lett.* **2014**, *104*, 251911.
(32) Messina, R.; Ben-Abdallah, P.; Guizal, B.; Antezza, M. Graphene-based amplification and tuning of near-field radiative heat transferbetween dissimilar polar materials. *Phys. Rev. B: Condens. Matter Mater. Phys.* **2017**, *96*, 045402.
(33) van Zwol, P. J.; Thiele, S.; Berger, C.; de Heer, W. A.; Chevrier, J. Nanoscale radiative heat flow due to surface plasmons in graphene and doped silicon. *Phys. Rev. Lett.* **2012**, *109*, 264301.
(34) Liu, X. L.; Zhang, Z. M. Giant enhancement of nanoscale thermal radiation based on hyperbolic graphene plasmons. *Appl. Phys. Lett.* **2015**, *107*, 143114.
(35) Ramirez, F. V.; Shen, S.; McGaughey, A. J. H. Near-field radiative heat transfer in graphene plasmonic nanodisk dimers. *Phys. Rev. B: Condens. Matter Mater. Phys.* **2017**, *96*, 165427.
(36) Renwen, Y.; Manjavacas, A.; García de Abajo, F. J. Ultrafast radiative heat transfer. *Nat. Commun.* **2017**, *8*, 2.
(37) Rodriguez-Lopez, P.; Tse, W. K.; Dalvit, D. A. R. Radiative heat transfer in 2D Dirac materials. *J. Phys.: Condens. Matter* **2015**, *27*, 214019.
(38) Mas-Bastellé, R.; Gómez-Navarro, C.; Gómez-Herrero, J.; Zamora, F. 2D materials: to graphene and beyond. *Nanoscale* **2011**, *3*, 20−30.
(39) Nikitin, A. Y.; Garcia-Vidal, F. J.; Martin-Moreno, L. Analytical expressions for the electromagnetic dyadic Green's function in graphene and thin layers. *IEEE J. Sel. Top. Quantum Electron.* **2013**, *19*, 4600611.
(40) Falkovsky, L. A. Optical properties of graphene. *J. Phys.: Conf. Ser.* **2008**, *129*, 012004.
(41) Low, T.; Chaves, A.; Caldwell, J. D.; Kumar, A.; Fang, N. X.; Avouris, P.; Heinz, T. F.; Guinea, F.; Martin-Moreno, L.; Koppens, F. Polaritons in layered two-dimensional materials. *Nat. Mater.* **2017**, *16*, 182−194.
(42) Abraham Ekeroth, R. M.; García-Martín, A.; Cuevas, J. C. Thermal discrete dipole approximation for the description of thermal emission and radiative heat transfer of magneto-optical systems. *Phys. Rev. B: Condens. Matter Mater. Phys.* **2017**, *95*, 235428.
(43) Koh, Y. K.; Bae, M.-H.; Cahill, D. G.; Pop, E. Reliably counting atomic planes of few-layer graphene ($n > 4$). *ACS Nano* **2011**, *5*, 269−274.
(44) Marcuse, D. *Theory of Dielectric Optical Waveguides*; Academic Press: London, 1991.
(45) Rodriguez, A. W.; Reid, M. T. H.; Johnson, S. G. Fluctuating-surface-current formulation of radiative heat transfer: theory and applications. *Phys. Rev. B: Condens. Matter Mater. Phys.* **2013**, *88*, 054305.
(46) Reid, M. T. H.; Johnson, S. G. Efficient computation of power, force and torque in BEM scattering calculations. *IEEE Trans. Antennas Propag.* **2015**, *63*, 3588−3598.
(47) Sadat, S.; Meyhofer, E.; Pramod, P. Resistance thermometry-based picowatt-resolution heat-flow calorimeters. *Appl. Phys. Lett.* **2013**, *102*, 163110.
(48) Zheng, J.; Wingert, M. C.; Dechaumphai, E.; Chen, R. Sub-picowatt/Kelvin resistive thermometry for probing nanoscale thermal transport. *Rev. Sci. Instrum.* **2013**, *84*, 114901.
(49) Low, T.; Roldán, R.; Wang, H.; Xia, F.; Avouris, P.; Martín-Moreno, L.; Guinea, F. Plasmons and screening in monolayer and multilayer black phosphorus. *Phys. Rev. Lett.* **2014**, *113*, 106802.
(50) Saito, Y.; Iwasa, Y. Ambipolar insulator-to-metal transition in black phosphorus by ionic-liquid gating. *ACS Nano* **2015**, *9*, 3192−3198.

DOI: 10.1021/acsphotonics.8b00328
ACS Photonics 2018, 5, 3082−3088